Studies of Male Reproduction in the Greater Bilby *Macrotis lagotis*

SD Johnston[1*], C Rumph[1], M Lucht[1], D Stenzel[2], V Nicolson[3], D Blyde[4] and T Keeley[4]

[1]School of Animal Studies, The University of Queensland, Gatton, Qld 4343, Australia
[2]Analytical Electron Microscopy Facility, Queensland University of Technology, Brisbane, Queensland 4001, Australia
[3]Dreamworld, Coomera, Qld, 4209, Australia
[4]Taronga Western Plains Zoo, Dubbo, NSW 2830, Australia
*Author for correspondence - Dr Steve Johnston, School of Animal Studies, The University of Queensland, Gatton, QLD 4343, Australia; Phone - 61732026902; Fax - 61733655644; Email - stevejohnston@uqconnect.net

ABSTRACT

Despite its vulnerable conservation status there is scant information on male Greater Bilby *Macrotis lagotis* reproduction. Observations of gross anatomy revealed a testis to body weight ratio of 0.08 - 0.17% (n = 4), the presence of a carrot shaped prostate with an oblique coronal segmentation of ventral and dorsal orientated prostatic tissue, an elongated membranous urethra, two bulbourethral glands and a bifurcated urethra in the glans penis (n = 1). The testis contained a high proportion of Leydig tissue (37.5 ± 2.7%) and a seminiferous epithelial cell cycle (8 stages identified) with a predominance of pre-meiotic stages (61.4 %) and Sertoli cells with unusually large nuclei. A GnRH stimulation test conducted on four different intact sexually mature Bilbies using 2µg Buserelin resulted in maximal plasma androgen secretion 30 to 60 mins after injection. While steps of *M. lagotis* spermiogenesis were similar to those described in peramelid marsupials, the morphology of the Bilby spermatozoan at spermiation, was radically different to that of the bandicoot sperm cell. Similar to the bandicoot, *M. lagotis* spermatozoa in the corpus epididymidis dislocated their neck insertion from the primary implantation fossa, so that by the time the sperm cell had reached the cauda epididymidis, the acetabulum had migrated cranially into a secondary implantation fossa and the nucleus had become streamlined with respect to the flagellum. This study reports the first description of large crystalloid inclusions in the principal cells of the caput epididymidal epithelium, the significance of which remains unknown. Male Bilby reproduction reported in this study supports the present taxonomic position of the Thylacomyidae.

Key words: Greater Bilby, Thylacomyidae, Gross reproductive anatomy, Testicular histology, Spermiogenesis, Epididymal sperm maturation, Epididymal crystalloids and Androgen secretion

Introduction

The Greater Bilby *Macrotis lagotis* is a small omnivorous, solitary, nocturnal marsupial found in the arid and semi-arid regions of central Australia (Pavey 2006). It now occupies only 20% of its former range, primarily as a result of predation by introduced predators, competition from feral herbivores and environmental degradation (Kennedy 1992; Southgate 1994). Despite its listing as vulnerable on the Red Species List (IUCN), there is little information on the male reproductive biology of this species. One study documents the ultrastructure of both caput and cauda epididymidal spermatozoa (Johnston *et al.* 1995), and another describes the ultrastructure of spermatozoa from a single poorly fixed specimen (Harding *et al.* 1990).

The mature spermatozoon of *M. lagotis* has a number of unique features that distinguish it from the spermatozoa of its peramelid and dasyurid relatives including the bifurcated flagellar acetabulum and the presence of double-thickened membrane / microtubules in the dorsal-ventral circumferential aspects of the distal midpiece (Johnston *et al.* 1995). While the morphology of the mature *M. lagotis* spermatozoan is primarily dasyurid-like in possessing a large elongated nucleus with a flattened acrosome covering 2/5 of the nuclear surface, it is the ultrastructural changes that occur during epididymidal transit that point to its close peramelid phylogeny; during epididymal maturation the spermatozoa of both species dislocate the neck of the flagelleum from the distal primary implantation fossa to a more proximally located "secondary" implantation fossa, allowing the mid-piece to juxtapose tightly against the ventral nuclear groove of the sperm head resulting in a mature spermatozoon with an extremely "stream-lined" appearance (Johnston *et al.* 1995; Harding *et al.* 1990; Taggart *et al.* 1995).

Apart from limited information on *M. lagotis* sperm ultrastructure, there have been no studies of gross reproductive anatomy, testicular histology, spermiogenesis or androgen secretion in this species; consequently this paper will be used to present a systematic descriptive analysis of *M. lagotis* male reproduction collected opportunistically over the last 8 years from a combination of post-mortem

Theme edition of Australian Zoologist "*Ecology meets Physiology*", a Gordon Grigg festschrift, edited by Lyn Beard, Daniel Lunney, Hamish McCallum and Craig Franklin. Australian Zoologist Vol 35 (2) 2010.

material, testicular tissue obtained following castration for genetic management and live animals. This study will not only increase the fundamental knowledge of male reproductive biology of this vulnerable species, but also provide an insight into the phylogenetic position of the Peramelemorphia.

Materials and methods

Animals

Nine sexually mature male Queensland *Macrotis lagotis* (2 - 5y) were used during the course of this study from September 2000 to August 2007. Five animals (B1 - B5) were part of a captive breeding program based at Taronga Western Plains Zoo, Dubbo, NSW and four were located in captivity in southeast Queensland at Dreamworld (B6 - 4.7 years and B7 - 4.0 years) and Currumbin Wildlife Sanctuary (B8 - 5.5 years and B9 - 5.5. years). B1 and B6 were used for the gross anatomical study; B2, B3, B4 and B5 for studies of testicular histology and spermiogenesis; B1 was used to examine accessory gland histology, while B6, B7, B8 and B9 were used to examine testosterone secretion. B1 and B6 were euthanased associated with general ill thrift and chronic arthritis; all other animals were clinically healthy at the time of observation. B2, B3, B4 and B5 were castrated as part of genetic management program; individual body weight and age data for each of these animals is shown in Table 1. Anatomical studies were conducted opportunistically.

Gross reproductive anatomy and accessory gland histology

Of the bilbies used for gross anatomy, B1 was dissected immediately after euthanasia, whereas the B6 carcass was frozen-thawed before examination. Following dissection, the prostate and bulbourethral glands of B1 were fixed in 10% buffered formalin and processed for histological sectioning (4μm thick sections stained with haematoxylin and eosin) by the Veterinary Pathology Laboratory based at Taronga Zoo, Mosman, Australia and viewed under the light microscope for photomicroscopy.

Histology of the testis and epididymis

Immediately after the testis was removed from the scrotum, it was washed in room temperature saline (0.9% sodium chloride, Baxter Healthcare Pty Ltd, Toongabbie, NSW, Australia) and the tunic albuginea scored with a scalpel blade to allow penetration of Bouin's fixative (Fronine Pty Ltd, Riverstone, NSW, Australia) for 24 hours. The testes were then transferred to 10% buffered formalin (Fronine Pty Ltd, Riverstone, NSW, Australia) until further histological processing. Testes were prepared and processed for standard histological processing for light microscopy. Four 4 μm thick sections, cut approximately 100 μm apart, were prepared from each block and stained with Mayer's haematoxylin and eosin.

Table 1. Gross testicular and epididymal weight of four *Macrotis lagotis*

Animal ID	Bilby 2	Bilby 3	Bilby 4	Bilby 5
Age (y)	2	2	4	4
Body Wt (Kg)	1.74	1.88	1.99	1.86
Combined Testicular Wt (g)	2.97	3.05	1.68	3.14
Combined Epididymal Wt (g)	0.49	0.44	0.41	0.62
Testis Wt / Body Wt (%)	0.17	0.16	0.08	0.17

The seminiferous cycle and quantitative histology

Quantitative testicular histology was determined from 4 bilbies (B2, B3, B4 and B5). Seminiferous tubule diameters were measured and assessed on transverse cross-sectioned tubules only. Random samples of 25 tubules from each section (100 per testis) were measured using an Olympus BH2 light microscope at approximately 100X magnification using a calibrated micrometer eyepiece. Relative frequencies of the major cell types within the testis were also measured using an Olympus BH2 light microscope (Olympus, Japan) connected to a Panasonic colour CCTV video camera (Panasonic, Japan) with the image displayed on a Sony television screen. Attached to the front of the television screen was a clear acetate film with a Weibel randomised grid system (Weibel 1979) photocopied onto it. The Weibel grid contained 36 repeatable points that could be used for random sampling. A total of 1500 points were counted per animal. The categories of cells counted were: (1) seminiferous tubules (ST, sperm producing tissue), (2) Leydig cells (LC), (3) blood vessels (BV) and (4) connective tissue (CT, parenchymal and tunica albuginea). Stages of the seminiferous epithelial cycle were characterised based on tubular morphology, which accounted for the shape and location of the spermatid nuclei, presence of mitotic divisions and the cellular associations of seminiferous epithelium (von Ebner 1871; Curtis 1918; Roosen-Runge and Giesel 1950) and on the limited marsupial data available (Setchell and Carrick 1973; Phillips et *al* 2008). Once the various stages had been identified at 200X magnification they were digitally photographed using a Nikon camera (Model DS-5M; Nikon Corporation, Japan) attached to a personal computer installed with the ACT–2U software package (Nikon Corporation, Japan). The cross-sectional areas of 50 Sertoli cell nuclei viewed under 100X oil immersion lens were estimated based on the area of circle.

Transmission electron microscopy - thick and thin sections

Immediately following castration, the tunica albuginea of one testis was scored with a scalpel blade before it was emersed into a petri dish containing cold (4°C) 3% glutaraldehyde (ProSciTech, Australia) in 0.1M phosphate buffer with 6% sucrose and cut into 2mm^3 tissue cubes on a soft dental wax surface; epididymal tissue was prepared in a similar way (Johnston *et al.* 1995). After fixation for 2h, the tissue was subsequently rinsed in 0.1M phosphate buffer (pH 7.2) with 6% sucrose, post-fixed in 1% osmium tetroxide (ProSciTech, Australia) for 80 mins, dehydrated, and embedded in Spurr's resin (ProSciTech, Australia). Thick sections were cut at 1μm intervals by ultramicrotomy, stained with toluidine blue

in borax and observed under light microscopy. Ultra-thin sections were stained with uranyl acetate and lead citrate. Ultrathin sections were examined and photographed with a JEOL 1200EX or a Hitachi H-300 transmission electron microscope operating at 80KV and 75KV, respectively.

Scanning electron microscopy

Spermatozoa from the cauda epididymides were fixed as per the transmission electron microscopy tissue but prepared for scanning electron microscopy. After washing with cacodylate buffer, the samples were post-fixed in 1% aqueous osmium tetroxide (ProSciTech, Australia) for one hour, dehydrated in an ascending series of ethanol and critically point dried with a Denton Vacuum Critical Point dryer. Samples were sputter-coated with gold (Biorad SC500), prior to examination and digital image recording with a FEI Quanta 200 scanning electron microscope, operating at 10kV.

GnRH agonist stimulation test, venipuncture and androgen assay

The GnRH agonist buserelin (2μg; Receptal®, Intervet, Australia) was administered I.M. to 4 males (B6 - B9) while the animals were under general anaesthesia. A blood sample was collected immediately before injection of buserelin (T0) and 30, 60, 90, 120, 180 and 240 mins post injection. Blood samples (0.5 ml) were collected from the mid-ventral tail using a 25 g needle attached to a winged infusion set and a 1 ml syringe (Becton Dickinson, New Jersey). Blood was placed into 1 ml heparinized tubes (Becton Dickinson, New Jersey), centrifuged at 1600 g for 5 min, the plasma recovered and frozen stored at -20°C until hormone analysis. Plasma samples were analysed for androgen concentration by enzyme immunoassay according to the procedures described by Walker *et al.* (2002), using polyclonal antiserum raised in New Zealand white rabbits (T-R156/7; 1:10000) and horseradish peroxidase conjugated label (C. Munro, UC Davis, USA; 1:15000). The EIA was validated for M. *lagotis* plasma by demonstrating parallelism between dilutions of pooled plasma and the standard curve (Figure 1). To test for potential interference, a recovery was performed; a total of 92.1% (n = 4) of exogenous steroid added to a pool of plasma was accurately measured by the assay, ensuring an acceptable level of interference from the sample matrix. The intra-assay and inter-assay coefficient of variation was 2.7% and 4.1% (n = 3) respectively. The detection limit of the assay was 0.04 to 20.0 ng/mL. All samples were assayed in duplicate and diluted 1:16 in assay buffer. The androgen antibody R156/7 (C. Munro; UC Davis) cross reacted with testosterone 100%, 5 -dihydrotestosterone 57%, androstenedione 0.27%, and < 0.05% with all other steroids tested.

Results

Gross reproductive anatomy

Macrotis lagotis possess a pre-penile pendulous narrow-necked scrotum containing testicles within a non-pigmented tunica vaginalis. The combined weight of the ellipsoid testes ranged from approximately 0.08 to 0.17% of the body weight (Table 1). The tunica albuginea of the testis was non-pigmented and the head of the epididymidis was not fused to the tunic. The glans penis is completely cleft into two distinct urethrae (Figure 2). *Macrotis lagotis* possesses carrot shaped prostate with an elongated membranous urethra (Figure 2). There were two pairs of Cowper's glands or bulbourethral glands each joined to the urethra by a distinctive duct (Figure 2).

Quantitative testicular histology and the seminiferous cycle

The mean (± SEM) relative proportion of tissue types found in the four Bilby testes examined in this study contained 52.6 ± 2.4% seminiferous tubules, 0.8 ± 0.1% blood vessels, 9.1 ± 0.8% connective tissue and 37.5 ± 2.7% Leydig cells (Table 2; Figure 3). The mean

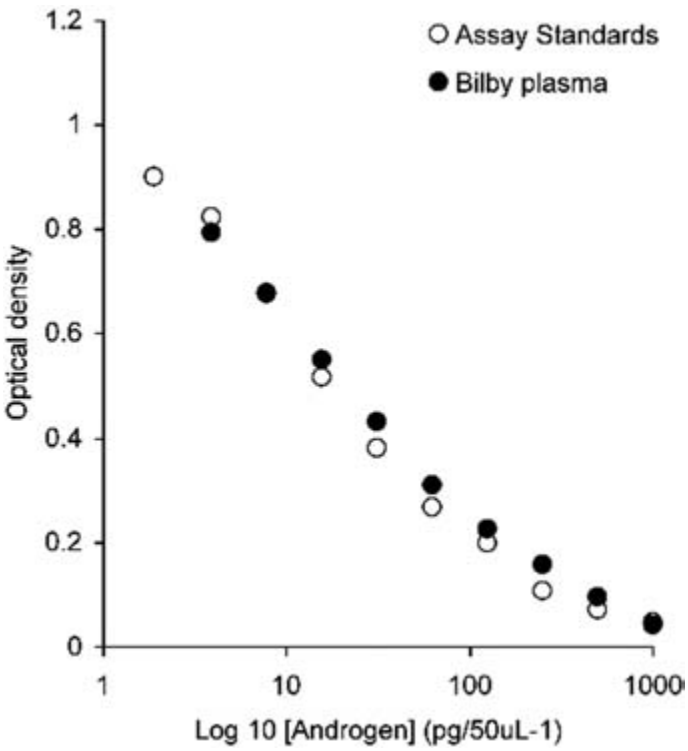

Figure 1. Parallelism of pooled *Macrotis lagotis* plasma androgen with the assay standards (Std).

Table 2. Relative percentage of tissue types found in the testis of four *Macrotis lagotis*

Animal ID	Bilby 2	Bilby 3	Bilby 4	Bilby 5	Mean ± SEM
% ST	60.4	51.3	48.0	50.5	52.6 ± 2.4
% LC	28.9	39.5	43.9	37.6	37.5 ± 2.7
% BV	0.8	1.0	0.8	0.7	0.8 ± 0.1
% CT	9.9	8.2	7.3	11.2	9.1 ± 0.8

ST – Seminiferous tubule; LC – Leydig cell; BV – Blood vessels; Ct – Connective tissue

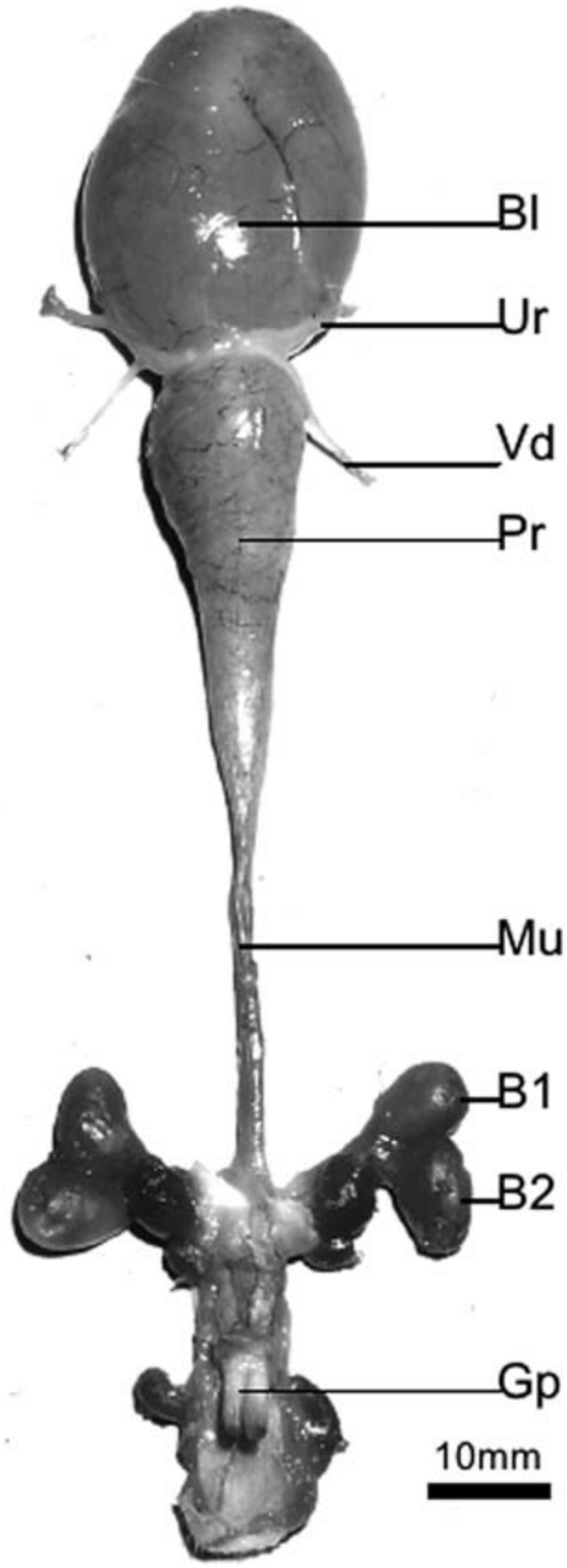

Figure 2. Gross male reproductive anatomy of *Macrotis lagotis*. B1 - bulbourethral gland 1; B2 - bulbourethral gland 2; Bl - bladder; Gp - glans penis; Mu - membranous urethra; Pr - prostate; Ur - ureter; Vd - vas deferens.

(± SEM) seminiferous tubule diameter of the 4 bilbies was 372.3 ± 15.5 μm. The mean (± SEM) Sertoli cell nuclear diameter and estimated cross-sectional area were respectively 18.9 ± 0.3 μm and 282 ± 7.6 μm^2.

A total of eight stages of the seminiferous cycle were categorised based on tubular morphology, although some of these stages (e.g. 8 and 1) were only subtly different and some inidividual cell types (e.g. intermediate spermatogonia and secondary spermatocytes) were difficult to clearly identify or rarely seen. The eight stages and their relative cellular associations are illustrated in figures 4 and 5.

Stage 1 of the seminiferous epithelial cycle contained type A spermatogonia that were present in all stages of the cycle and found adjacent to the basement membrane of tubule. Also aligned along the basement membrane were pre-leptotene spermatocytes, then an inner layer of pachytene primary spermatocytes and finally a luminal layer of round spermatids (3 to 4 cells deep). By stage 2, the preleptotene spermatocytes had given rise to leptotene spermatocytes and the pachytene primary spermatocytes were slightly more advanced (late pachytene; not shown in figure 4). However, the most characteristic feature of this stage of the cycle was the condensed but not completely flattened nucleus of the round spermatids. In stage 3 of the seminiferous cycle, the nucleus had elongated and flattened with respect to its long axis and was orientated parallel to the basement membrane of the tubule. In slightly more advanced stage 3 cellular associations, leptotene spermatocytes had transformed to a basal layer of zygotene spermatocytes adjacent to the basement membrane, while the inner layer of pachytene spermatocytes (2 cells deep) had developed into diplotene primary spermatocytes. Stage 4 was characterised by the presence of meiotic figures associated with the dividing primary spermatocytes; in some sections, smaller secondary spermatocytes (none shown in figure 4) were detected but these were rarely observed. During this stage, zygotene spermatocytes lined the basal compartment of the seminiferous tubule, while flattened

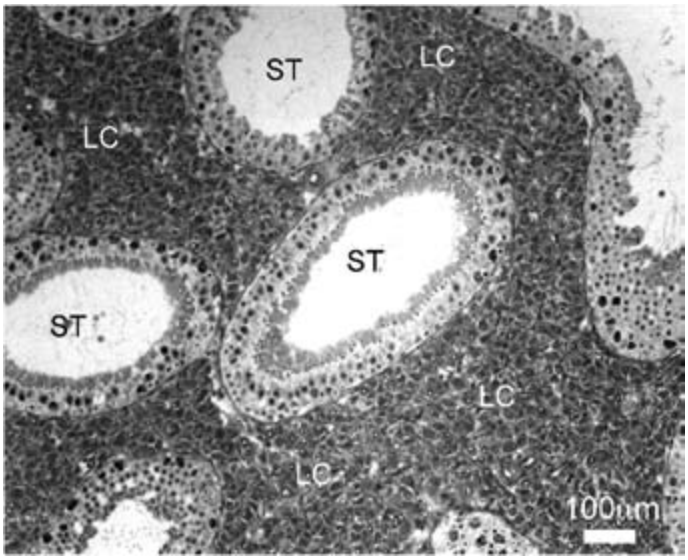

Figure 3. *Macrotis lagotis* testicular parenchyma histological section. Note the very high proportion of Leydig cell tissue compared to spermatogenic tissue in this section. LC - Leydig cell tissue; ST - Seminiferous tubule.

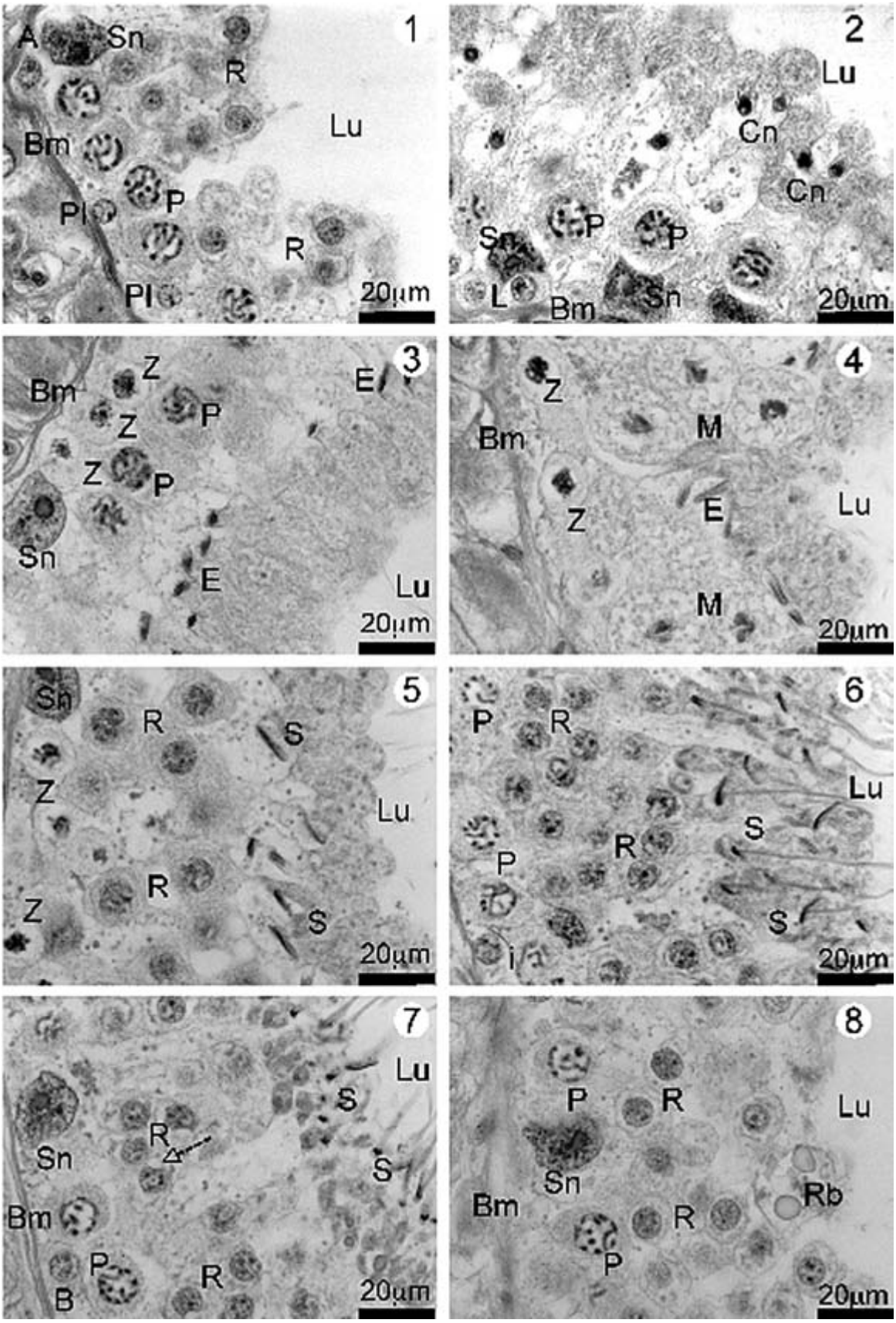

Figure 4. Histological sections of the stages (1–8) of the *Macrotis lagotis* seminiferous epithelial cycle based on tubular morphology. A - A spermatogonia; Bm - basement membrane; B - B spermatogonia; Cn - condensing spermatid; El, elongated flattened spermatid; i - intermediate spermatogonia; L - leptotene spermatocyte; Lc - Leydig cell; M - meiotic figures; P - pachytene spermatocyte; pL - pre-leptotene spermatocyte; R - round spermatid; Rb - residual body; S - spermatozoa; Sn - Sertoli cell nucleus; Z - zygotene spermatocyte; dashed arrow indicates early spermatid with an acrosomal vacuole.

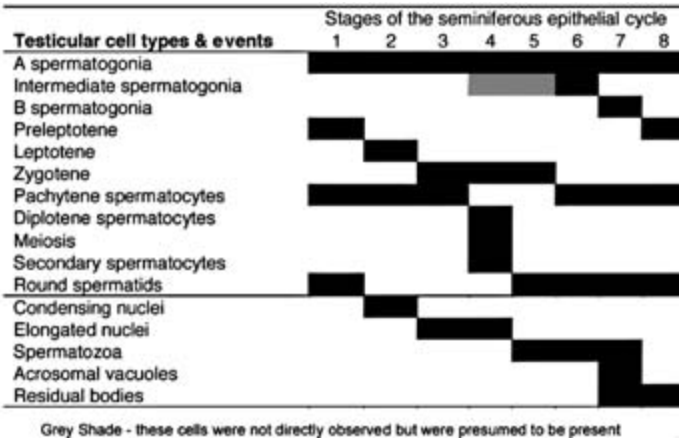

Figure 5. Summary and relative frequency of the stages of the Bilby seminiferous epithelial cycle based on tubular morphology.

elongated spermatids from the previous meiosis had transformed into recognizable spermatozoa with distinctive sperm heads and flagella, and were orientated in a range of positions relative to the basement membrane. Stage 5 of the Bilby seminiferous epithelial cycle had 2 layers of spermatids, a basal layer of spermatozoa with their nuclei orientated in a slightly oblique position relative to the flagellum and a freshly produced set of round spermatids. During this stage it was still possible to identify a uniform layer of zygotene spermatocytes on the basal edge of the tubule. Stage 6 was characterised by the re-appearance of pachytene primary spermatocytes that had transformed from zygotene spermatocytes. An inner layer of round spermatids was surrounded by a luminal layer of spermatozoa that had heads, which were orientated obliquely to the long axis of the flagella; the nuclei of the maturing spermatozoa now contained a large skirt of cytoplasm. Stage 7 tubules possessed spermatozoa lining the extreme luminal edge of the seminiferous tubule; the cytoplasmic skirt around the sperm head had regressed and in some sections it was possible to observe a residual layer of cytoplasm between the Sertoli cell and the sperm cell. The nuclei of these spermatozoa were rotated close to parallel with the long axis of the flagella. A layer of round spermatids was found adjacent the spermatozoal layer, behind which was a layer of pachytene spermatocytes and B-type spermatogonia. The round spermatids of stage 7 also possessed a large acrosomal vacuole, which had collapsed by stage 8. The final stage of the seminiferous epithelial cycle (stage 8) was primarily defined by spermiation and transition of B spermatogonia into pre-leptotene spermatocytes. Residual bodies, formed from the loss of spermatid cytoplasm, were also a prominent feature of this stage.

Pre-meiotic (8, 1 - 3) and post-meiotic (5 - 7) stages represented 61.4% and 35.7% of the seminiferous cycle respectively. Table 3 shows the frequency of each stage of the *M. lagotis* seminiferous epithelial cycle for individual animals (B2, B3, B4 and B5).

Spermiogenesis

Spermiogenesis in *M. lagotis* was classified into 6 stages primarily based upon the relative position and shape of the acrosome and nucleus as documented in the bandicoot (Sapsford *et al.* 1967; 1968); there were insufficient appropriate micrographs to fully describe the genesis of the flagellum and neck insertion. The spermatid in stage 1 (Figure 6A) was similar to that of other mammalian species in that it contained a large round uncondensed nucleus and a relatively small amount of cytoplasm. The Golgi body, which is the precursor of the marsupial acrosome, was characteristically positioned adjacent the round spermatid nucleus and numerous mitochondria were found evenly distributed within the cytoplasm. The centrioles in latter stage 1 (not shown) had migrated to the ventral pole of the spermatid nucleus.

The spermatid nucleus remained round and uncondensed during stage 2 but membrane vesicles arose from the Golgi body and fused to form the acrosomal vacuole (Figure 6B). As the acrosomal vacuole increased in size it protruded into the cranial aspect of the nucleus, forming a characteristic "V" shape indentation. At this point, electron dense material, destined to form the acrosome, had accumulated in the centre of this indentation.

Stage 3 of spermiogenesis was characterised by the spermatid nucleus migrating or protruding towards the acrosomal membrane, which resulted in the collapse of the acrosomal vacuole, sandwiching of the nuclear envelope and plasma membrane and the early stages of the "Sertoli cell reaction". At this stage, the nucleus had taken on a cone-shaped appearance, the manchette was well developed and the chromatin had started to become patchy; nuclear pores had also developed at the base of the nucleus alongside a basal thickening of the membrane, under which can be seen an electron dense structure that would ultimately become the annulus; limited observations of nuclear protrusion in *M. lagotis* suggest that this stage maybe relatively brief.

Table 3. Mean (± SEM) relative frequencies of the stages of the Bilby seminiferous cycle (n = 4)

Stage of SC	Bilby 2	Bilby 3	Bilby 4	Bilby 5	
1	13.5	7.8	8.9	7.5	9.4 ± 0.5
2	9.4	12.7	16.0	12.7	12.7 ± 1.3
3	33.1	34.2	35.6	30.1	33.4 ±1.2
4	3.9	2.2	2.2	3.2	2.9 ± 0.4
5	1.4	2.8	4.0	2.0	2.3 ± 0.6
6	17.9	18.1	14.3	21.4	18.0 ± 1.5
7	15.8	15.1	14.3	16.2	15.4 ± 0.4
8	5.1	7.0	4.7	6.9	5.9 ± 0.6

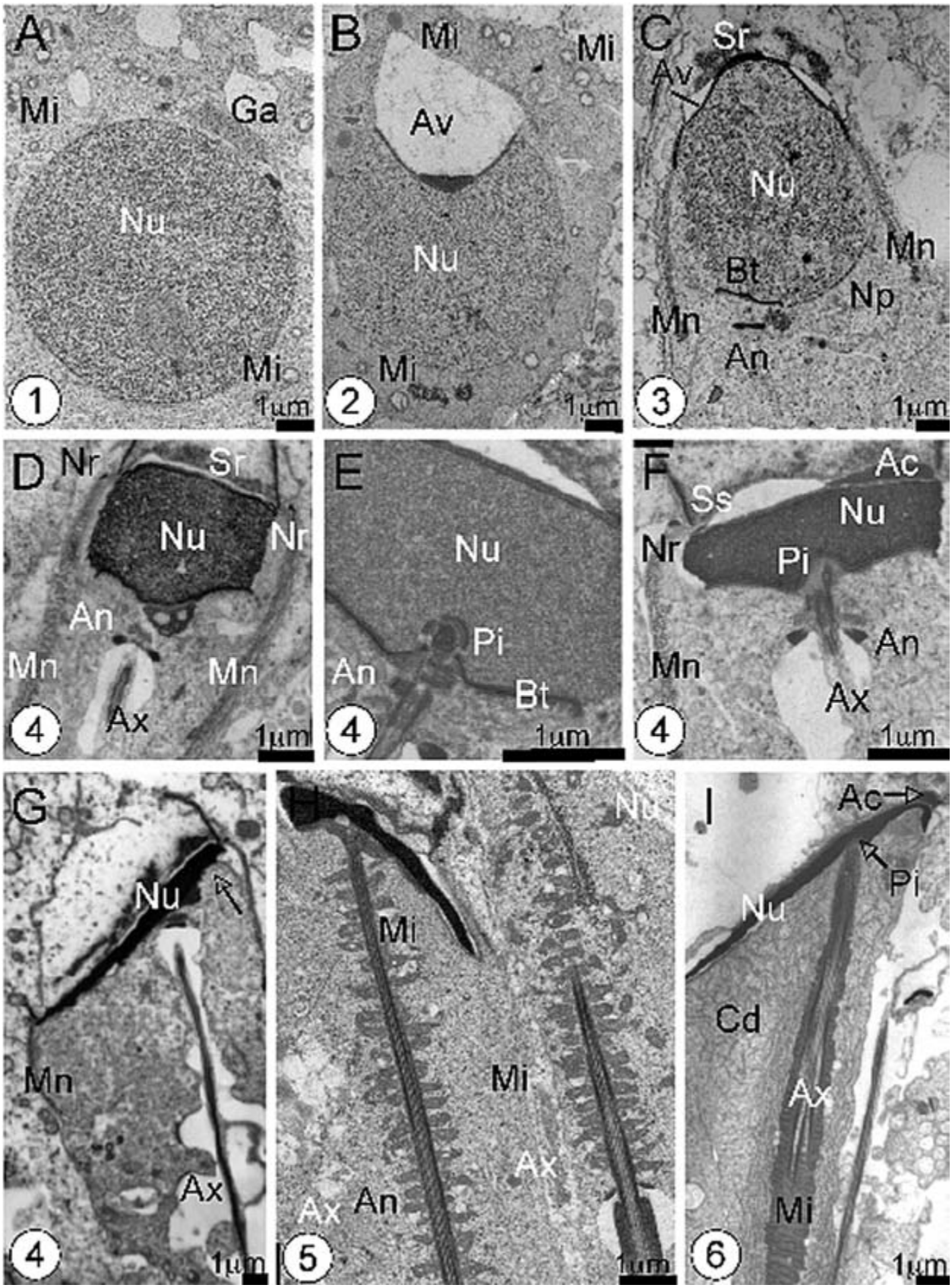

Figure 6. Stages (1 - 6) of spermiogenesis in *Macrotis lagotis* as shown by transmission electron microscopy. A - stage 1; B - stage 2; C - stage 3; D - early stage 4; E - mid stage 4; F - late stage 4; G - stage 5; H - stage 6; I - spermiation; Ac - acrosome; An - annulus; Ax - axoneme; Av - acrosomal vacuole; Bt - basal thickening; Cd - cytoplasmic droplet; Ga - golgi apparatus; Mi - mitochondria, Mn - manchette; Nu - nucleus; Np = nuclear pores; Nr - nuclear ring; Pi - primary implantation fossa; Sr - Sertoli cell reaction; Ss - Sertoli cell spur.

Stage 4 (Figure 6D-G) of spermiogenesis was categorised by significant chromatin condensation and a dorsal-ventral flattening of the nucleus. Figures 6D-G indicate the progressive condensation and flattening of the nucleus and the gradual formation of the acrosome. There was a series of recognisable intermediate phases in stage 4 of spermiogenesis. In the earliest of these phases the nucleoplasm had started to condense and flatten to take on a characteristic rectangular shape (Figure 6D). At this point of development the dorsal and ventral membranes of the nucleus were thickened and there was an indentation in the medial ventral membrane that would ultimately give rise to the primary implantation fossa. The nuclear membrane around the lateral aspect of the sperm head was not thickened and was only loosely adhered to the nucleoplasm. It was possible to clearly see the microtubules of the manchette on the lateral extremities of the spermatid, the associated nuclear ring and the Sertoli cell spurs that extend into the Sertoli cell cytoplasm and an electron dense region along the dorsal surface of the acrosome known as the Sertoli cell reaction. During this stage, acrosomal material was being deposited on the dorsal nuclear surface and some sections showed an asymmetrical accumulation of acrosomal contents that would eventually form the bulk of this structure; at this stage of development the annulus had also began its distal descent. The middle phase of stage 4 spermiogenesis was primarily characterised by further nuclear condensation and flattening and continued development of the structures associated with the connecting piece and implantation fossa (Figure 6E and 6F). The acrosome during this phase was located asymmetrically on the dorsal-lateral aspect of the flattening nucleus; the remaining dorsal surface of the nucleus was covered with the remnants of the collapsing acrosomal vacuole. Mitochondria were still present at the base of the spermatid cytoplasm and had yet to gather around the axoneme. The end of stage 4 was characterised by further condensation and flattening of the nucleus (Figure 6G). The lateral margins of the sperm nucleus at the end of stage 4 appeared crenulated (almost degenerative in nature), as did the nucleoplasm surrounding the implantation fossa; the nucleus at this point was orientated in an oblique position relative to the flagellum.

In stage 5 (Figure 6H), the nucleus continued its rotation about the primary implantation fossa so that by the end of this phase it was orientated approximately 45° to the longitudinal axis of the flagellum. Stage 5 was also clearly identified by the presence and alignment of numerous mitochondria along the longitudinal axis of the anterior region of the axoneme to give the characteristic formation of the mid-piece; the mitochondria were not tightly packed into a helical whorl at this stage. A small acrosomal vacuole was still present over the dorsal distal nuclear surface and acrosome – the anterior thickened region of the acrosome had become bulbous in appearance.

Stage 6 of spermiogenesis was spermiation (Figure 6I) where the mature spermatid was liberated from the seminiferous epithelium into the lumen. At spermiation, the axoneme was inserted into the primary implantation fossa, the acrosomal vacuole of stage 5 had collapsed further and the mitochondria were now fully tightened around the axoneme in a series of whorls. The spermatozoa were released into the lumen of the seminiferous tubule with excess cytoplasm and the cytoplasmic droplet contained various organelle and cytoplasmic debris (Figure 6I).

Androgen secretion

All bilbies treated with GnRH agonist showed an increase in their plasma androgen concentration with 60 mins of injection and this remained elevated over the 240 min observation period (Figure 7). However, there was individual animal variation in response to the GnRH agonist, with B7 showing only a small increase in androgen concentration above that of the non-stimulated level.

Caput epididymal crystalloid inclusions

Crystalloid inclusions were found primarily in principal cells throughout the caput epithelium; none were found in the corpus or cauda epididymides. Crystalloid inclusions occupied approximately 1/5 to 1/2 of the size the epithelial cell cytoplasm; the size and shape of the crystalloid was extremely variable (Figure 8A and 8C). All crystalloid inclusions where confined within the cytoplasm of the epithelial cells in the caput epididymidis. The mean (± SD) length of the crystalloid was 8.9 ± 6.7 μm and the mean (± SD) width 2.2 ± 1.2 μm. The mean (± SD) periodicity or distance between the lines of the crystal lattice network (Figure 8D) within the crystalloid inclusions was 9.0 ± 1.3 nm; some of the crystalloid inclusions were surrounded by ribosomes. Crystalloid inclusions were identified in both young (2 years) and older animals (4 years). The crystalloid inclusions in some sections (Figure 8B) appeared to have had a devastating effect on the epithelial cells of the caput epididymidis; in some cases they had ruptured the cell membrane and distorted the majority of the epithelial architecture to the point where the epithelium appeared highly degenerative. In other sections, the crystalloid inclusion had a broken or fragmented appearance (Figure 8C).

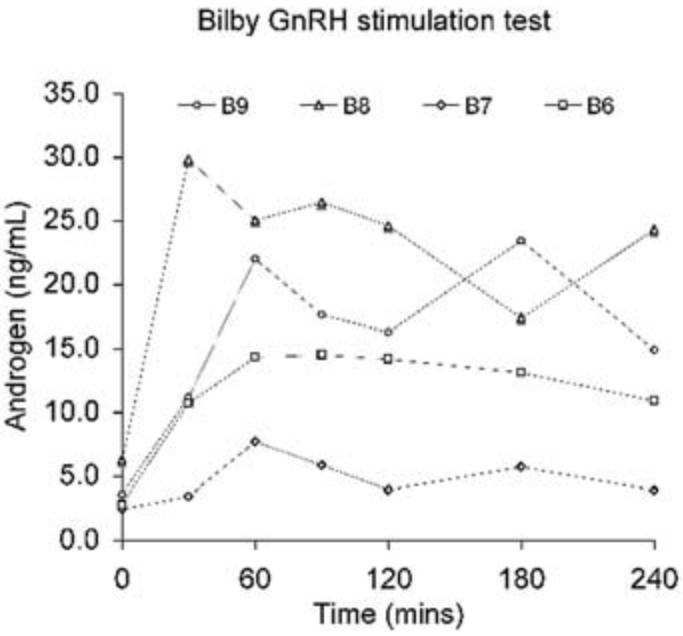

Figure 7. Androgen secretion (ngmL−1) in individual male ***Macrotis lagotis*** following administration of 2µg of the GnRH agonist buserelin.

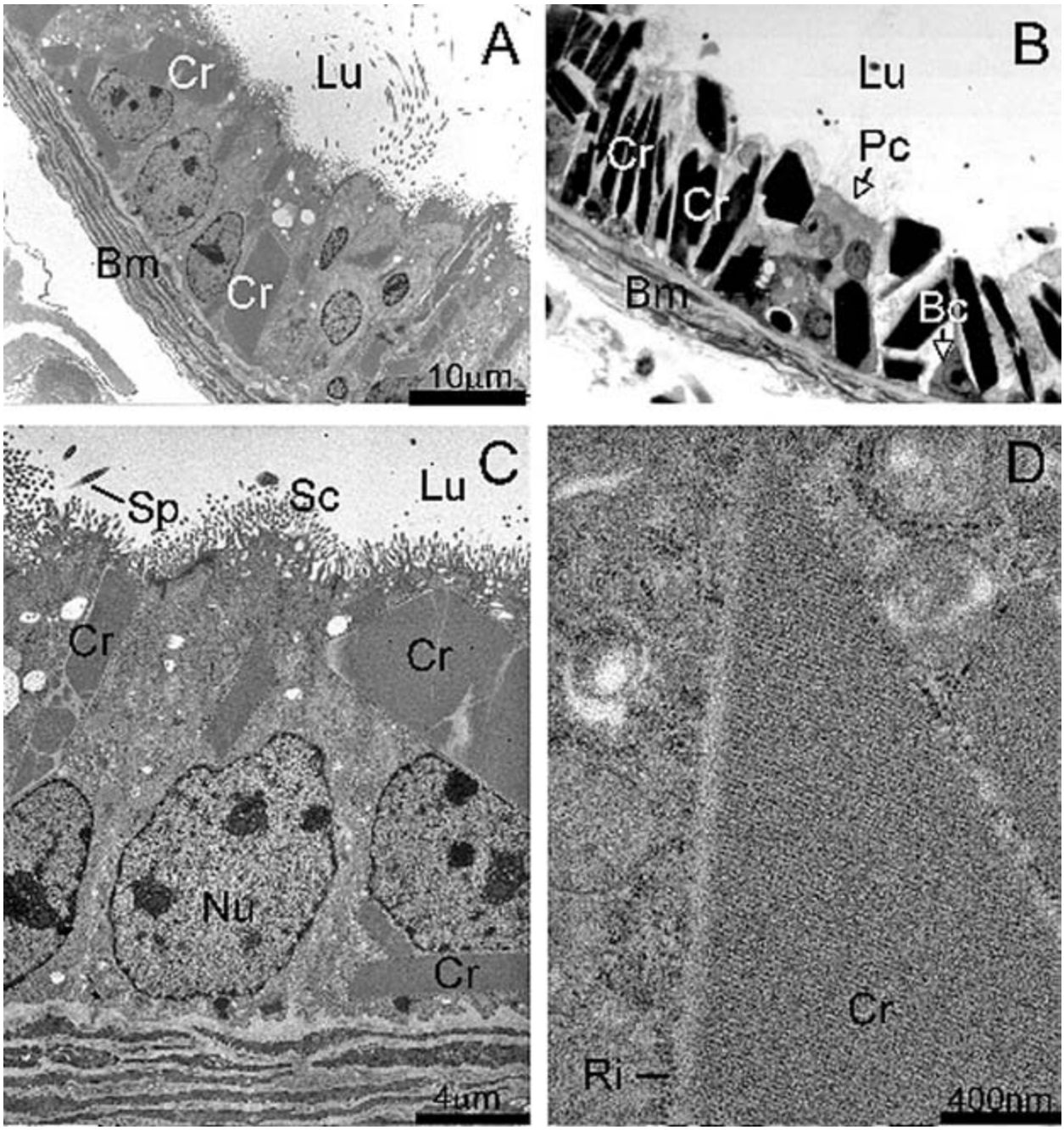

Figure 8. *Macrotis lagotis* epididymal histology and crystalloid inclusions. A - Low power transmission electron micrograph of caput epididymal epithelium showing presence of crystalloid inclusions; B - Low power light micrograph demonstrating crystalloid inclusions within the caput epididymal epithelium; C - High power transmission electron micrograph of the caput epididymal epithelium showing presence of crystalloid inclusions; D - Fine structure of a crystalloid inclusion within the caput epididymal epithelium; Bc - Basal cells; Cr - crystalloid inclusion; Lu - lumen; Nu - nucleus; Pc - principal cell; Ri - ribosomes; Sc - stereocilia; Sp - spermatozoa.

Epididymal maturation

When the spermatozoon leaves the testis and enters into the caput epididymidis, the capitulum of the neck of the flagellum was inserted into the primary implantation fossa (Figure 9A) connected by electron dense material (Figure 9B). In this position, the sperm head was essentially parallel to the flagellum but it was not completely streamlined in appearance and there was a large cytoplasmic droplet present. As the spermatozoa enter into the corpus epididymidis, the neck insertion was still associated with the primary implantation fossa (Figure 9C) but there was evidence that the capitulum of the neck had become dislocated from the fossa (Figure 9D); the cytoplasmic droplet was still present at this point. By the time the sperm cell had entered into the cauda epididymidis, the capitulum had completely disassociated from the primary implantation fossa and had migrated cranially into the inner curvature of the sperm head (Figure 9E and 9F); this migration allowed the nucleus (ventral groove) to align tightly against the flagellum; consequently, the mature spermatozoon had an extremely streamlined appearance (see Figures 10A-D). *Macrotis lagotis* sperm chromatin was also very susceptible to decondensation when air-dried (Figure 10E) suggesting a probable lack of cysteine residues in the sperm protamines.

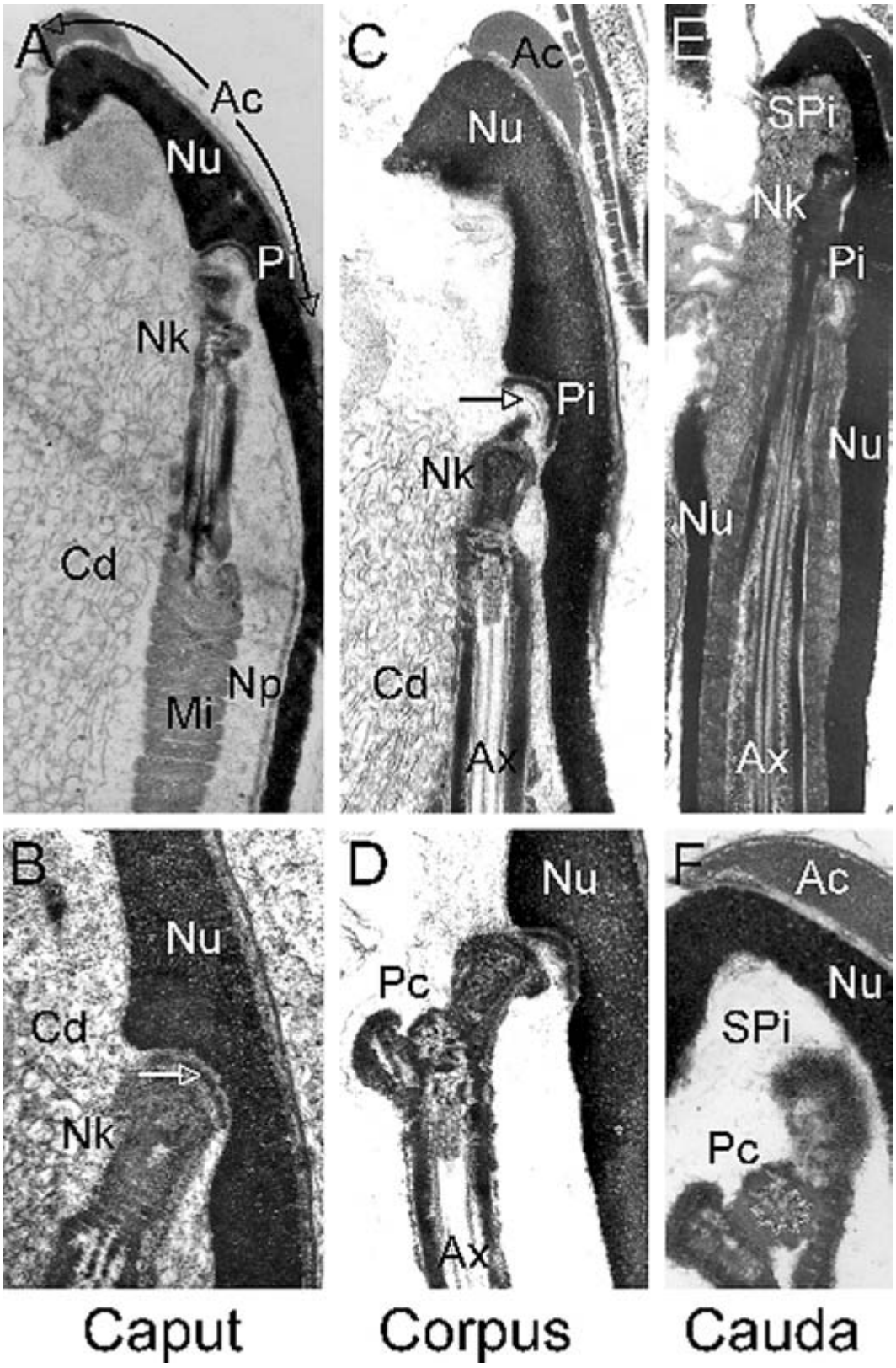

Figure 9. Changes to the neck insertion of Bilby spermatozoa during epididymal transit as shown by transmission electron microscopy. A - Saggital section through a caput epididymidal spermatozoon; B - Saggital section through neck insertion of a caput epididymidal spermatozoon; C - Saggital section through a corpus epididymidal spermatozoon; D - Saggital section through neck insertion of a corpus epididymidal spermatozoon; E - Saggital section through a cauda epididymidal spermatozoon; F - Saggital section through neck insertion of a cauda epididymidal spermatozoon; Ac - acrosome; Ax - axoneme; Cd - cytoplasmic droplet; Mi - mitochondria; Nk - neck region of the flagellum; Nu - nucleus; Np - nuclear pores; Pc - proximal centriole; Pi - primary implantation fossa; Spi - secondary implantation fossa; black arrow - neck region dislocated from the primary implantation fossa; white arrow - electron dense material cementing the capitulum of the neck of the flagellum to the implantation fossa.

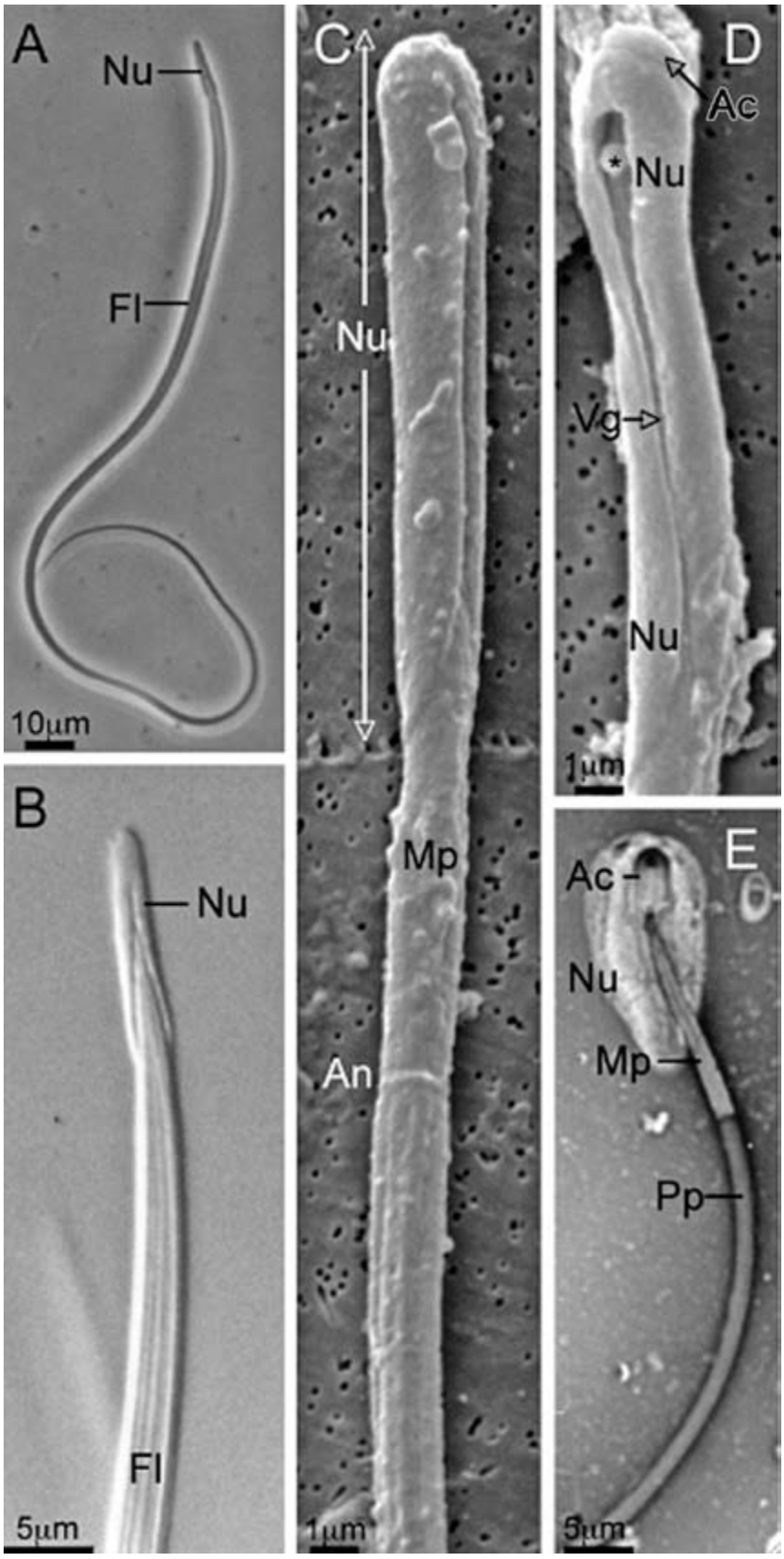

Figure 10. *Macrotis lagotis* mature cauda epididymidal spermatozoa. A - phase contrast micrograph of a whole spermatozoon; B - Nomarski differential interference micrograph of the sperm head and midpiece; C - Scanning electron micrograph of sperm head and midpiece; D - Scanning electron micrograph highlighting the ventral groove and one arm of the neck capitulum ; E - Brightfield micrograph of air-dried sperm showing decondensed sperm chromatin and refractile acrosome. Ac - acrosome; An - annulus; Fl - flagellum; Mp - midpiece; Nu - nucleus; Vg - ventral groove; * - capitulum of the axoneme neck region.

Accessory gland (prostate and bulbourethral gland) histology

The carrot shaped Bilby prostate (Figure 11A) was composed of 2 distinctive glandular tissue types or segments; these shall be referred to as dorsal and ventral regions (Figure 11B-D). In the cranial transverse portion of the prostate, the ventral tissue type pre-dominated but caudally this changed so that at the caudal distal extremity of the prostate, the dorsal tissue was the dominant type. The dorsal tissue consisted of dilated glands composed of a single low layer of columnar to cuboidal epithelium filled with a clear acellular fluid. The ventral tissue consisted of many single branched tubular glands (varying in their degree of dilation) that were constructed from a single layer of tall columnar cells and filled with eosinophilic acellular granular material.

Macrotis lagotis possessesd two sets of bulbo-urethral glands that collected into a single duct that subsequently drained into the membraneous urethra at the base of the penis. The bulbo-urethral gland consisted of single branched tubular glands with wide lumina composed of a single low layer of columnar to cuboidal epithelium filled with an acellular eosinophilic secretion. At the base of the bulbourethral gland there were numerous tubules that joined to empty into a collecting duct that was composed of columnar epithelium.

Discussion

This study represents the first general description of the male reproductive biology of the Bilby. Although the taxonomic position of the Thylacomyidae has been controversial (Groves and Flannery 1990; Baverstock *et al.* 1990) it is generally considered to have a close (Perameloidea) but divergent phylogenetic relationship to the Peramelidae (Clemens *et al.* 1989; Johnson 1989; Pacey *et al.* 2001); consequently, the following discussion will explore evidence for this relationship using the information reported here on male Bilby reproduction.

The most distinctive features of the gross reproductive anatomy of the male Bilby when compared to the Peramelidae are the shape of the prostate and the complete bifurcation of the distal urethra and glans penis (Owen, 1868). The prostate of *M. lagotis* is clearly carrot shaped as that found in the majority of marsupials and therefore dissimilar to the distinctive heart shape previously reported for the Northern brown bandicoot *I. macrourus* and Long-nosed bandicoot *Perameles nasuta* (Rodger and Hughes 1973). In addition, while *M. lagotis* had the same basic histological segmentation of ventral and dorsally orientated prostatic tissues as that found in the bandicoots (Rodger and Hughes 1973), the precise topographical distribution of these tissues was different. The Bilby prostate possesses an oblique coronal segmentation of the ventral and dorsal tissues, so that the cranial component is predominantly ventral tissue and caudal component is composed of primarily dorsal tissue. *Macrotis lagotis* and bandicoots, do however, share an elongated membranous urethra. The functional significance of the dual urethrae in the glans penis requires further investigation but may be related to the separate deposition of spermatozoa into the two lateral vaginae; McCracken (1990) has described separate vaginal caeca and a vaginal cul-de-sac with the presence of a persistent medial septum in nulliparous and parous bilbies.

There are only 2 bulbo-urethral glands in *M. lagotis*, a feature also shared with the bandicoots (*P. nasuta,* Eastern barred bandicoot *Perameles gunni* and *I. macrourus*), Long-nosed potoroo *Potorous tridactylus,* Brushtail Possum *Trichosurus vulpecula,* Tasmanian Devil *Sarcophilus harrisii* and Fat-tailed Dunnart *Sminthopsis crassicaudata* (Rodger and Hughes, 1973). The testicular to body weight ratio for *M. lagotis* of 0.17 was substantially lower than that reported for *Isoodon obesulus* (0.38) and the majority of other marsupials e.g. *M. lagotis* is ranked 3rd lowest of the 13 species previously described by Short RV (unpublished data in Tyndale-Biscoe and Renfree 1987).

The average proportion Leydig cell volume observed within the testis of *M. lagotis* (37.5%) was similar to that observed in the testis of the Koala (*Phascolarctos cinereus,* 33%; Johnston unpublished observations) and Swamp Antechinus (*Antechinus minimus*, 23–37%; Wilson and Bourne 1984) but substantially higher than that reported for the Common Ringtail Possum (*Pseudocheirus peregrinus,* 12.6%, Phillips *et al.,* 2008), Common Wombat (*Vombatus ursinus*, 14.6%, MacCallum, 2005), South American White-belly Opossum (*Didelphis albiventris*,12.5%; Queiroz and Nogueira 1992) and *I. macrourus* (21%; Todhunter and Gemmell 1987). The Bilby, Koala and Swamp Antechinus clearly fit into a collection of non-phylogenetically aligned species which Fawcett *et al.* (1973) defined as group 3 and which have abundant closely packed Leydig cells that occupy nearly all the enlarged intertubular areas, but which have little connective tissue and very few interstitial lymphatics. While Todhunter and Gemmell (1987) have reported a seasonal increase in the percentage of Leydig cell tissue of the bandicoot testis coming into the breeding period from approximately 9% to 21%, seasonal changes in the proportion of Leydig cells in the Bilby testis are unknown, although we do know that they breed throughout the year in captivity (Jackson 2003). Interestingly, 44% of the testicular parenchyma of Bilby B4 was Leydig cell tissue and this is one of the highest Leydig cell proportions published for a marsupial. While the significance of such a high proportion of Leydig cells is perplexing, it has been speculated that a similar high proportion of interstitial tissue in the testis of eutherian species (e.g. domestic boar) may be associated with a high androgen or oestrogen secretion or the production of odoriferous steroids that serve as pheromones (Fawcett *et al.,* 1973).

The mean diameter of the seminiferous tubules found in the Bilby was 372.3 μm and was similar to that of the only other bandicoot species described (*P. nasuta*, 370 - 450 μm; Woolley 1990) and in the middle of the range reported for marsupials generally (Setchell 1977). Sertoli cell nuclei in the Bilby testis were unusually large and only slightly smaller in cross-sectional area to that reported for *P. cinereus* (Temple-Smith and Taggart, 1990); the Koala and Bilby Sertoli cell nuclei were approximately 3X the size of those found in *Antechinus*

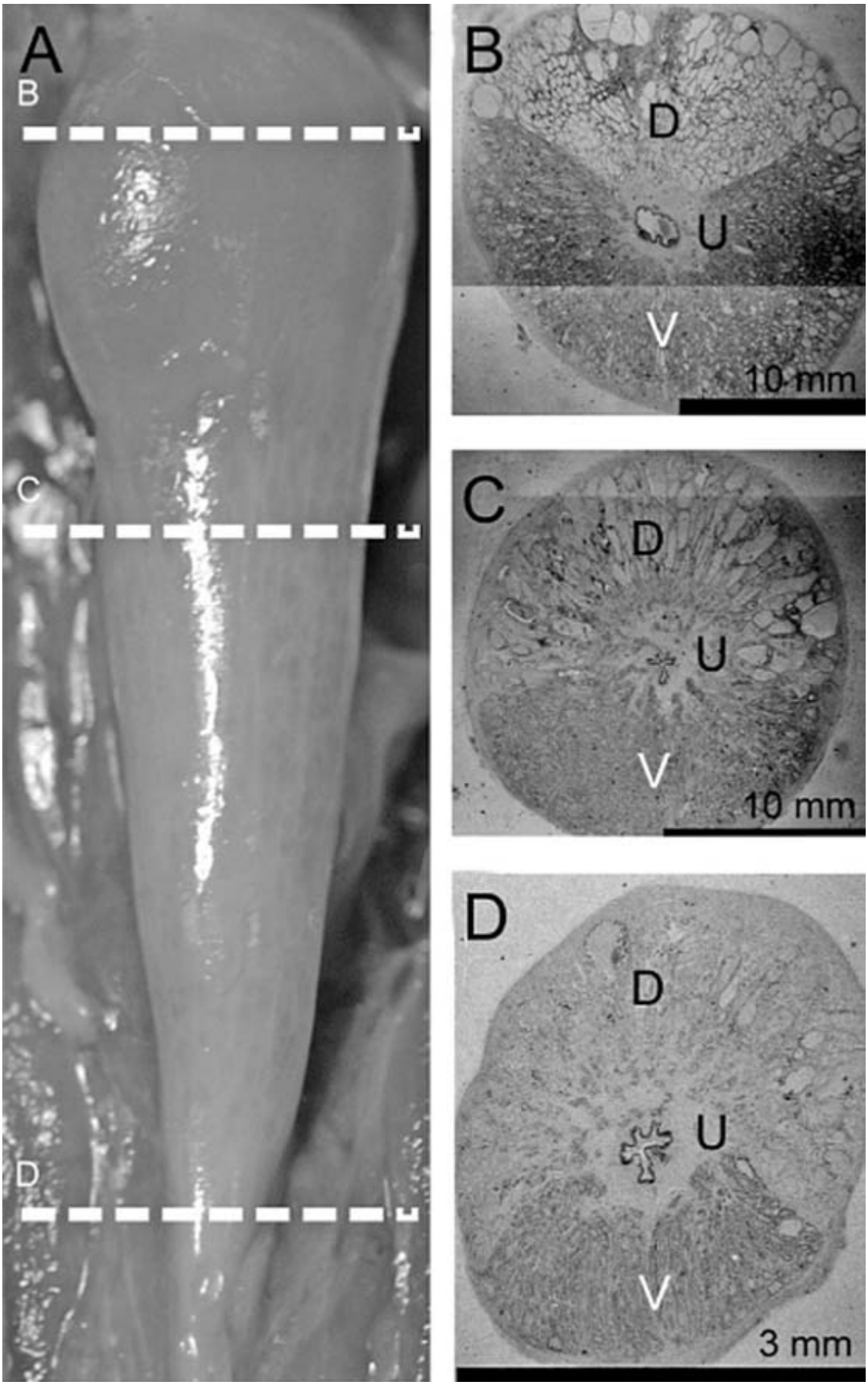

Figure 11. *Macrotis lagotis* prostate gross anatomy and tissue segmentation. A - Gross anatomy of prostate; B-D representative transverse histological sections of the Bilby prostate. D - dorsal prostatic tissue; U - urethra; V - ventral prostatic tissue.

stuartii and 5X as large as those reported in eutherian species (Temple-Smith and Taggart, 1990). Despite the similarity in the size of the Sertoli cell nucleus, the Bilby Sertoli cell cytoplasm did not contain the unusual crystalloid structures present in Koala Sertoli cells (Kerr *et al.* 1987). Shea (2001) has also described large Sertoli cell nuclei in Australian snake, *Ramphotyphlops nigrescens* but commented that the biological significance of these large nuclei is unknown.

The eight tubular stages of the seminiferous epithelial cycle in the Bilby were fundamentally similar to the cellular associations previously described for the small number of marsupials that have been investigated (Setchell and Carrick 1973; Setchell 1977; Phillips *et al*. 2008); nevertheless, there were some minor variations in the definitions of the stages that need to be highlighted. For example, it should be noted that Mason and Blackshaw (1973) had previously described (without accompanying figures) the spermatogenic cycle of *I. macrourus* but only identified six stages of the cycle based on nuclear morphology and cellular association; some stages reported by Mason and Blackshaw (1973) could readily be further subdivided to give the more traditional 8 stages as identified by Phillips *et al*. (2008) in *Pseudocheirus peregrinus* e.g. stage 1 into stages 8 (spermiation) and 1 and stage 5 into stages 5 and 6 - stage 6 of Mason and Blackshaw (1973) would then become stage 7 of Phillips *et al.* (2008). It should be noted that while the classification system used to stage the seminiferous cycle for the Bilby was slightly different to that used by Setchell and Carrick (1973) when staging the Tammar Wallaby *Macropus eugenii, Macropus rufogriseus, T. vulpecula* and *P. nasuta*, these differences were only arbitrary. It is also important to note that while Lin *et al*. (2004) have recently described the seminiferous epithelial cycle of *T. vulpecula* based on the progressive development of the spermatid, this approach is not directly comparable to the tubular morphology classification system used in the present study.

Setchell and Carrick (1973) defined two categories into which marsupials can be grouped in terms of the relative frequencies of the various stages of the seminiferous cycle. The first category has animals in which the pre-meiotic stages of the cycle are more frequent than those following meiosis and include the *M. rufogriseus*, *P. nasuta* and *T. vulpecula*, whereas the second category is the reverse of this phenomenon and is represented by *M. eugenii* and *P. peregrinus* (Phillips *et al*. 2008). Results of this study have shown that Bilby belongs to the first category with 61% of the seminiferous epithelial cycle pre-meiotic.

Spermiogenesis in *M. lagotis* was essentially similar to that described in the *P. nasuta* (Sapsford *et al.* 1967; 1968; Setchell 1977) with some slight variations on the mechanisms with respect to the categorising of the various stages and the shape of the sperm nucleus and acrosome. Sapsford *et al.* (1967) defined stage 1 or the early spermatid stage in the bandicoot from the earliest form of the round spermatid to the point of development of the acrosomal vacuole; in the Bilby we sub-divided this stage into 2, a stage 1 to describe the round spermatid in the pre-acrosomal vacuole stage and a stage 2 to describe the round spermatid during the formation of the acrosomal vacuole. Stage 3 in Bilby spermiogenesis is the nuclear protrusion stage and is equivalent to stage 2 of bandicoot spermiogenesis as described by Sapsford *et al*. (1968); this stage appears to be very brief in the Bilby. Stage 4 of spermiogenesis in *M. lagotis* can be referred to as nuclear flattening or condensation and is the same as stage 3 in the bandicoot. Stage 5 of Bilby spermiogenesis occurs when the nucleus undergoes a rotation about its point of attachment so that it comes to lay approximately 45° to the longitudinal axis of the flagellum - in the bandicoot this is defined as stage 4 (Sapsford *et al.* 1968). Stages 5 and 6 in the bandicoot are known as the early and late post-rotational stages respectively. Stage 5 begins when the annulus begins to move distally and terminates when the early mitochondrial sheath of the middle piece has been formed (Sapsford *et al*. 1968). No major changes occur to the nuclear morphology of the spermatozoa in stage 6 but they do migrate to the lumen where they are shed in the process of spermiation. These spermiogenic processes also occur in the Bilby but we have combined early and late post-rotation stages into a single post-rotational stage 6 and recognised spermiation as end of this phase. The final shape of the mature testicular sperm head and acrosome in the Bilby is radically different to that of the bandicoot, being over twice the length and covering 2/5 of the cranial and dorsal aspects of the nucleus respectively (Johnston *et al*. 1995).

The GnRH stimulation test conducted on *M. lagotis* in this study resulted in a sustained secretion of androgen such that after 30 to 60 min post-injection, the concentration of androgen in all 4 animals was elevated compared to their pre-stimulation level and then remained elevated over the subsequent 3h observation period. It would, therefore, appear that 2μg of buserelin I.M. is sufficient to provide a reliable time dependent index of the steroidogenic capacity of the testis in the Bilby; equally the GnRH agonist stimulation test could also be used to evaluate the steriodogenic capacity of the testis coming into puberty or any seasonal change in male reproductive function.

While the fundamental cytology and ultrastructure of the *M. lagotis* epididymis was unremarkable when compared to other marsupials (Tyndale-Biscoe and Renfree 1987), the caput epididymides of all 4 bilbies showed evidence of crystalloid inclusions. Although crystalloids have been described in the Sertoli Cell of the Koala testis (Kerr *et al*. 1987), the crystalloids described here in *M. lagotis* have never been reported in the epididymis of a marsupial. Despite repeated attempts to determine the basic chemical composition of the crystalloid from fixed material embedded in resin (C. Rumph and S.D. Johnston unpublished observations), further analysis with appropriately fixed or fresh material is required.

Crystalloid structures have been identified in the caput epididymis of the Marmoset *Callithrix jacchus* (Asuk Humar *et al*. 1990) and rat (Sawatzke and Heidger 1977), within the corpus epididymidis of the nine-banded Armadillo *Dasypus novemcinctus mexicanus* (Edmonds and

Nagy 1973) and in the cauda epididymidis of the dog (Gouranton *et al*. 1979; Sawatzke and Heidger 1977), stallion (Gouranton *et al*. 1978) and vas-sectomised rats (Sawatzke and Heidger 1977) but no pathological effect was discussed. The crystalloids in this study were identified in the principal cells of the caput epididymidis of *M. lagotis* and not membrane bound so that they bore no resemblance to those described in the marmoset or rat. Asuk Humar *et al*. (1990) have suggested that the inclusions may be involved in steroidogenic activity, while Edmonds and Nagy (1973) and Sawatzke and Heidger (1977) have noted that the number of crystalloids increases with the age of the animal. The crystalloid inclusions identified in the Bilby caput epididymis were found in both young (2y) and older (4y) animals; although no comparative quantitative counts of crystalloids where made between bilbies, there appeared to be a greater incidence of the pathology in the older animals. It is possible that the crystalloids are a result of precipitation of an intercellular substance caused during the fixation or embedding procedure for transmission electron microscopy, but this seems unlikely, as crystalloids were not evident in the corpus or cauda epididymides and sections of caput epididymidal epithelium that did not contain crystalloids showed evidence of being appropriately fixed. Despite the apparent epididymal pathology associated with the crystalloid inclusions, the testis and corpus and cauda epididymis of all 4 bilbies contained significant numbers of what appeared to be normal spermatozoa. In addition, sperm recovered from the cauda epididymidis of these animals and diluted into a Tris-citrate buffer (S.D. Johnston, unpublished observations) showed evidence of progressive motility.

As previously reported by Johnston *et al*. (1995) the capitulum of the Bilby sperm disconnects from the implantation fossa during epididymal maturation and migrates cranially into the terminal portion of the nuclear groove; this arrangement allows the connecting piece and the cranial portion of the midpiece close apposition up against the ventral nuclear grove and thereby aligns the sperm nucleus into a highly hydrodynamic arrangement. TEM observations in this study have revealed that the capitulum does not disconnect from the primary implantation fossa until it enters the corpus epididymidis. It is interesting to note that spermatozoa in the corpus epididymidis still possess a cytoplasmic droplet; perhaps the cranial movement of the flagellum into what has been termed a secondary implantation fossa (Johnston *et al*. 1995) may be associated with the removal of the cytoplasmic droplet. Taggart *et al*. (1995) have reported that a similar dislocation of the neck and migration of the flagellum in *I. macrourus* was associated with changes to a vacuole and fine filament connecting structures on the leading edge of the connecting piece; while it is possible that the Bilby spermatozoon has a similar mechanism of flagellum migration, no such connecting structures were detected in this study. Following migration of the flagellum, there does not appear to be a strong physical connection between the sperm head and flagellum so that the sperm head / flagellum connection is likely to be susceptible to breakage. Preliminary observations of sperm cryopreservation of cauda epididymidal spermatozoa have revealed an increased number of "decapitated" heads following freeze-thaw procedures (S.D. Johnston unpublished observations); *Macrotis lagotis* sperm chromatin also appears to be susceptible to relaxation following cryopreservation (S.D. Johnston unpublished observations) and following the preparation of air-dried eosin-negrosin stain smears in this study.

The results of this study have shown that while the *M. lagotis* shares a number of its male reproductive characteristics in common with the Peramelidae (prostate tissue segmentation, elongated membranous urethra, 2 bulbo-urethral glands, diameter of the seminiferous tubule, percentage of pre-meiotic stages of the seminiferous cycle, dislocation of sperm neck insertion to a more cranial position in the ventral nuclear groove during epididymal transit) there are clearly significant phenotypic differences that set it apart from the bandicoots (gross prostate shape, lower testis to body weight ratio, bifid urethra in glans penis, 2X higher Leydig cell volume in the testis, large Sertoli cell nuclei, presence of crystalloids in the caput epididymal epithelium and a range of sperm ultra-structure apomorphies [see Johnston *et al*., 1995]) and which continue to support its present taxonomic status.

Acknowledgements

This work was conducted under the authority of the University of Queensland's AEC committee (SAS/358/07) and was in part financially supported by the Save the Bilby Fund.

References

Asuk Humar R., Ojha, P.P., Anand Kumar T.C. 1990. Ultrastructure of paracriny/steroidogenesis in principal cells of the marmoset epididymis. *Archives of Andrology* **24**: 167-75.

Baverstock, P.R., Flannery, T., Aplin K., Birrell, J. and Krieg, M. 1990. Albumin immunological relationships of the bandicoots (Perameloidea: Marsupialia) - a preliminary report. Pp. 13 - 18 in *Bandicoots and Bilbies,* edited by. J.H. Seebeck, P.R. Brown, R.L. Wallis and C.M. Kemper. Surrey Beatty and Sons Pty Ltd, Sydney, NSW.

Clemens, W.A., Richardson, B.J. and Baverstock, P.R. 1989. Biogeography and phylogeny of the Metatheria. In *Fauna of Australia. Mammalia*, Vol. 1B., edited by D.W. Walton and B.J. Richardson. Australian Government Publishing Service, Canberra, ACT.

Curtis, G.M. 1918. The morphology of the mammalian seminiferous tubule. *American Journal of Anatomy* **24**: 339–94.

Edmonds, R.H. and Nagy, F. 1973. Crystalloid inclusion bodies in the epididymis of the Nine-banded Armadillo, *Journal of Ultrastructure Research* **42:** 82-6.

Fawcett, D.W., Neaves, W.B. and Flores, M.N. 1973. Comparative Observations on Intertubular Lymphatics and the Organisation of the Interstitial Tissue of the Mammalian Testis. *Biology of Reproduction* 9: 500-532.

Gouranton, J., Folliot, R. and Thomas, D. 1978. The crystalloid intranuclear inclusions of the stallion epididymis. *Journal of Submicroscopic Cytology*, **10:** 309-14.

Gouranton, J., Folliot, R. and Thomas, D. 1979. Fine structure and nature of the crystalloid intracellular and intracytoplasmic inclusions in dog cauda epididymis, *Journal of Ultrastructure Research* **69:** 273-8.

Groves, C.P. and Flannery, T. 1990. Revision of the Families and Genera of Bandicoots. Pp. 1 - 11 in *Bandicoots and Bilbies,* edited by. J.H. Seebeck, P.R. Brown, R.L. Wallis and C.M. Kemper. Surrey Beatty and Sons Pty Ltd, Sydney, NSW.

Harding, H.R. Shorey, C.D. and Cleland, K.W. 1990. Ultrastructure of spermatozoa and epididymal maturation in perameloids. Pp. 235-50 in *Bandicoots and Bilbies* edited by J.H. Seebeck, P.R. Brown, R.L. Wallis and C.M. Kemper. Surrey Beatty and Sons Pty Ltd, Sydney, NSW.

Jackson, S.M. 2003. Bandicoots. Pp. 127-44 in *Australian Mammals: Biology and Captive Management* edited by S. Jackson. CSIRO, Collingwood, Victoria.

Johnson, K.A. 1989. Thylacomyidae. Pp. 625-635 in *Fauna of Australia, Mammalia* Vol. 1B edited by D.W. Walton and B.J. Richardson. Australian Government Publishing Service, Canberra, ACT.

Johnston, S.D. Daddow, L. and Carrick, F. 1995. Ultrastructural and light microscopic observations of mature epididymal spermatozoa and sperm maturation of the Bilby, *Macrotis lagotis* (Metatheria, Mammalia), *Memoire-du-Museum-National-d'Histoire-Naturelle* **166:** 397-407.

Kennedy, M. 1992. *Australasian Marsupials and Monotremes: an Action Plan for Their Conservation.* IUCN: Gland, Switzerland.

Kerr, J.B., Knell, C.N. and Irby, D.C. 1987. Ultrastructure and possible function of giant crystalloids in the Sertoli cell of the juvenile and adult Koala *(Phascolarctos cinereus). Anatomy and Embryology* **176**:213-34.

Lin, M., Harman, A., and Fletcher, T.P. 2004. Cycle of the seminiferous epithelium in a marsupial species, the brushtail possum (*Trichosurus vulpecula*) and estimation of its duration. *Reproduction Fertility and Development* **16**: 307–13.

Mason, K. and Blackshaw, A, 1973. The spermatogenic cycle of the bandicoot, *Isoodon macrourus*. *Journal of Reproduction and Fertility* (Abstract) **32**: 307.

McCracken, H.E. 1990. Reproduction in the Greater Bilby, *Macrotis lagotis* (Reid) - a comparison with other perameloids. Pp. 199-204 in *Bandicoots and Bilbies*, edited by H. Seebeck, P.R. Brown, R.I. Wallis, and C.M. Kemper. Surrey Beatty and Sons, Sydney, NSW.

MacCallum, C.A. 2005. The Reproductive Biology of the Common Wombat, *Vombatus ursinus*: Studies towards the development of an artificial insemination protocol. *Masters of Philosophy Thesis*, The University of Queensland.

Owen, R. 1868. *On the Comparative Anatomy and Physiology of Vertebrates*, *Vol III Mammals*, pp. 760-775. London: Longmans, Green.

Pacey, T.L., Baverstock, P.R. and Jerry, D.R. 2001. The phylogenetic relationships of the Bilby, *Macrotis lagotis* (Peramelimorphia: Thylacomyidae), to the bandicoots - DNA sequence evidence. *Molecular Phylogenetics and Evolution* **21**: 26-31.

Pavey, C. 2006. National Recovery Plan for the Greater Bilby *Macrotis lagotis*. Northern Territory Department of Natural Resources, Environment and the Arts.

Phillips, D.J., McKinnon, A., Keeley, T. and Johnston, S.D. 2008. Testosterone secretion, testicular histology and the cryopreservation of cauda epididymidal spermatozoa in the common ringtail possum (*Pseudocheirus peregrinus*) *Reproduction, Fertility and Development* **20**: 391–401.

Queiroz, G. F. and Nogueira, J. C. 1992. Duration of the cycle of the seminiferous epithelium and quantitative histology of the testis of the South American white-bellied opossum (*Didelphis albiventris*), Marsupialia. *Reproduction Fertility and Development* **4**: 213–22.

Rodger, J.C. and Hughes, R.L. 1973. Studies of the accessory glands of male marsupials. *Australian Journal of Zoology*, **21:** 303-20.

Roosen-Runge, E. C., and Giesel, L. O. 1950. Quantitative studies on spermatogenesis in the albino rat. *American Journal of Anatomy* **87**: 1–23.

Sapsford, C.S., Rea, C.A. and Cleland, K.W. 1967. Ultrastructural studies on spermatids and Sertoli cells during early spermiogenesis in the bandicoot *Perameles nasuta* Geoffroy (Marsupialia). *Australian Journal of Zoology* **15**: 881-909.

Sapsford, C.S., Rae, C.A. and Cleland, K.W. 1968. Ultrastructural studies on the maturing spermatids and on Sertoli cells in the Bandicoot *Perameles nasuta Geoffroy* (Marsupialia). *Australian Journal of Zoology* **17:** 195 – 292.

Sawatzke, C.L. and Heidger, Jr. P.M. 1977. Ultrastructure of crystalloid inclusions in the dog and rat epididymis, *Tissue and Cell*, **9:** 733-44.

Setchell, B.P. 1977. Reproduction in male marsupials. Pp. 411-57 in *The Biology of Marsupials*, edited by B. Stonehouse and D. Gilmore. University Park Press, London.

Setchell, B. P., and Carrick, F.N. 1973. Spermatogenesis in some Australian marsupials. *Australian Journal of Zoology* **21**: 491-9.

Shea, G.M. 2001. Spermatogenic cycle, sperm storage, and Sertoli cell size in a Scolecophidian (Ramphotyphlops nigrescens) from Australia. *Journal of Herpetology* **35**: 85-91.

Southgate, R.I. 1994. Why introduce the Bilby? Pp. 165-170 in *Reintroduction Biology of Australian and New Zealand Fauna* edited by M. Serena. Surrey Beatty and Sons, Sydney, NSW.

Taggart, D.A. Leigh, C.M. and Breed, W.G. 1995. Ultrastructure and motility of spermatozoa in the male reproductive tract of perameloid marsupials. *Reproduction Fertility and Development* **7**: 1141-56.

Temple-Smith, P.D. and Taggart, D.A. 1990. On the male generative organs of the Koala (*Phascolarctos cinereus*), an update. Pp. 33-54 in *Biology of the Koala*, edited by A.K. Lee, K.A. Handasyde and G.D. Sanson, Surrey Beatty and Sons Pty Ltd, Sydney, NSW.

Todhunter, R. and Gemmell, R.T. 1987. Seasonal changes in the reproductive tract of the male marsupial bandicoot, *Isoodon macrourus*. *Journal of Anatomy* **154**: 173-86.

Tyndale-Biscoe, C.H. and Renfree, M. 1987. *Monographs on Marsupial Biology*, *Reproductive Physiology of Marsupials*, University of Cambridge Press, Cambridge.

von Ebner, H. 1871. Untersuchunge über den bau de samekanälchen und die entwickling der spermatozoiden bei den säugethieren ind beim menschen. *Untersuch. Inst. Physiol. Histol. Graz* **2**: 200–236.

Walker, S.L., Waddell, W.T. and Goodrowe, K.L. 2002. Reproductive endocrine pattern in captive female and male red wolves (*Canis rufus*) assessed by fecal and serum hormone analysis. *Zoo Biology* **21**: 321–35.

Weibel, E.R. 1979. *Stereological Methods. Vol.1: Practical Methods for Biological Morphometry*. Academic Press: London.

Wilson, B.A. and Bourne, A.R. 1984. Reproduction in the male dasyurid *Antechinus minimus maritimus* (Marsupialia: Dasyuridae). *Australian Journal of Zoology* **32**: 311–8.

Woolley, P.A. 1990. The seminiferous tubules, rete testis and efferent ducts in peramelid marsupials. Pp. 229-34 in *Bandicoots and Bilbies,* edited by. J.H. Seebeck, P.R. Brown, R.L. Wallis and C.M. Kemper. Surrey Beatty and Sons Pty Ltd, Sydney, NSW.